Three-coordinate copper(II) with halide ligands is normal

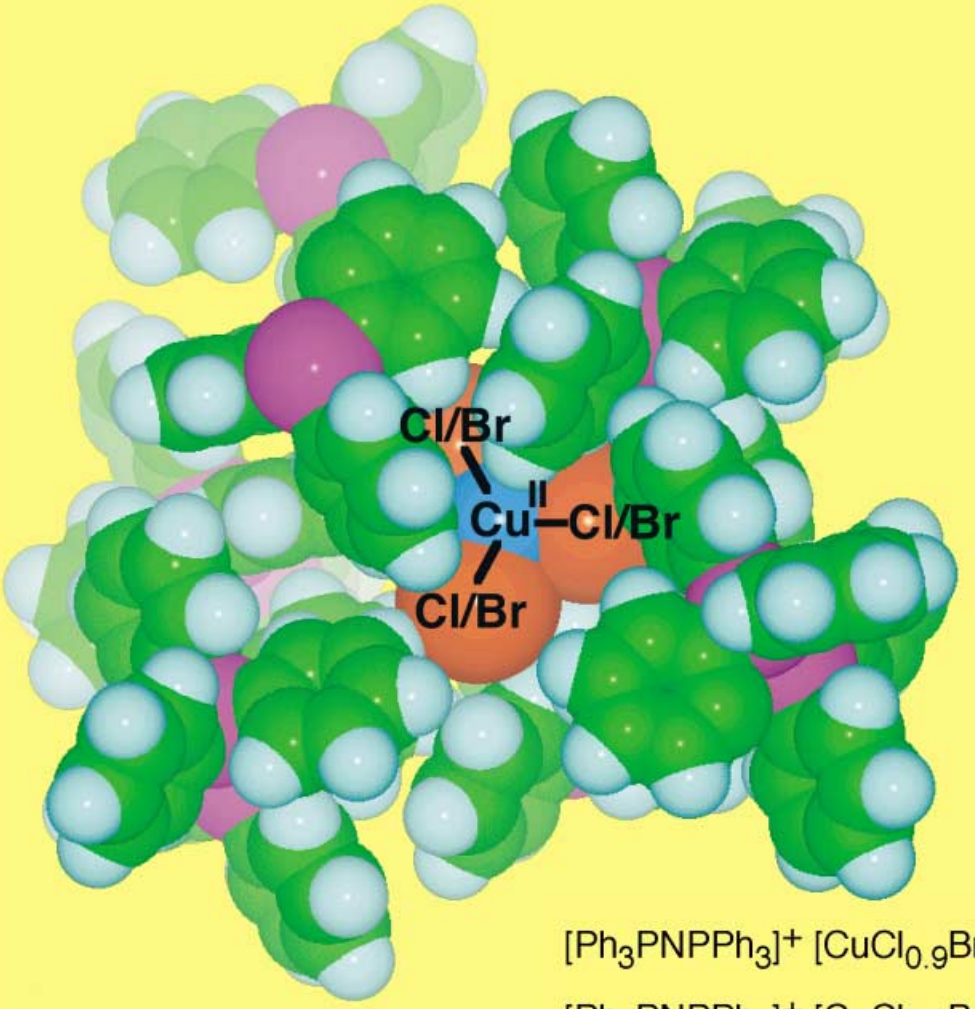

$[Ph_3PNPPh_3]^+ [CuCl_{0.9}Br_{2.1}]^-$

$[Ph_3PNPPh_3]^+ [CuCl_{2.4}Br_{0.6}]^-$

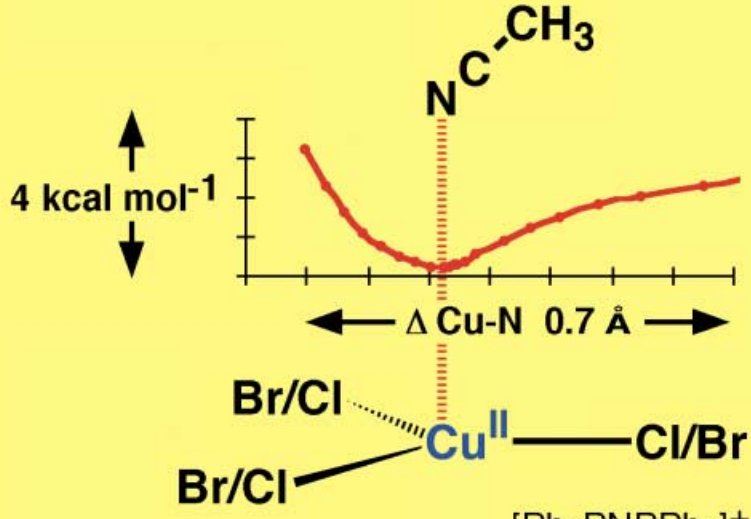

$[Ph_3PNPPh_3]^+ [CuCl_{0.7}Br_{2.3}(NCCH_3)]^-$

For more information see the following pages.

 © WILEY-VCH Verlag GmbH, 69451 Weinheim, Germany, 2002 0947-6539/02/0806-1269 $ 17.50+.50/0

Three-Coordinate $[Cu^{II}X_3]^-$ (X = Cl, Br), Trapped in a Molecular Crystal

Catrin Hasselgren,*[a] Susan Jagner,*[a] and Ian Dance*[b]

Abstract: Mixtures of $[Ph_3PNPPh_3]^+Cl^-$ with $CuBr_2$ (or $CuBr_2 + CuCl_2$) in ethanol/dichloromethane yield crystals containing three-coordinate copper(II) with mixed chloride and bromide ligands, namely $[Ph_3PNPPh_3]^+[CuCl_{0.9}Br_{2.1}]^-$ (**1**) and $[Ph_3PNPPh_3]^+[CuCl_{2.4}Br_{0.6}]^-$ (**2**). The trigonal-planar coordination of copper(II) is angularly distorted but unambiguous, as there is no other halide ligand within 6.7 Å of the copper atom. Density functional theory (DFT) calculations on planar $[CuClBr_2]^-$ show that the energy surface for angle bending is very soft. Crystallisation in the presence of CH_3CN yields $[Ph_3PNPPh_3]^+[CuCl_{0.7}Br_{2.3}(NCCH_3)]^-$ (**3**), in which there is additional secondary coordination by $NCCH_3$ (Cu–N 2.44 Å). DFT calculations of the potential energy surface for this secondary coordination show that it is remarkably flat (< 3 kcal mol^{-1} for a variation of Cu–N by 0.8 Å). The crystal packing in **1**, **2** and **3**, which involves multiple phenyl embraces between $[Ph_3PNPPh_3]^+$ ions and numerous C–H···Cl and C–H···Br motifs, is associated with intermolecular energies that are larger than the variations in intramolecular energies. For reference, the crystal structures of $[Ph_3PNPPh_3^+]_2[Cu_2Cl_6]^{2-}$ (**4**) and $[Ph_3PNPPh_3^+]_2[Cu_2Br_6]^{2-}$ (**5**) are described. We conclude 1) that three-coordinate copper(II) with monatomic halide ligands, although uncommon, can be regarded as normal, 2) that steric control by ligands is not necessary to enforce three-coordination, 3) that a hydrophobic aryl environment stabilises $[Cu(Cl/Br)_3]^-$, and 4) that the energy change in the transition from three- to four-coordinate copper(II) is very small (ca 5 kcal mol^{-1}).

Keywords: copper · coordination modes · crystal packing · density functional calculations · halides

Introduction

Copper(II) complexes are generally four-, five- or six-coordinate and display various coordination geometries, often distorted. Three-coordinate Cu^{II} is rare and is best known and studied in the copper protein sites of type 1, in which the coordination number varies between 3 and 4 in association with electron transfer between Cu^{II} and Cu^{I}.[1, 2] For Cu^{I}, three-coordination is relatively common, as are four- and two-coordination. It is notable that a 1999 review[3] of three-coordinate transition metal complexes reported that Cu^{I} has more instances of three-coordination in the Cambridge structural database (CSD) than any other transition metal, but that the CSD then contained no instance of three-coordinate Cu^{II}. Recently, the first small molecules containing trigonally coordinated Cu^{II} were prepared and characterised, as CuLY: they involve the bidentate ligand L, with Cl or $SCPh_3$ as the third ligand Y (Scheme 1).[4, 5] Some steric protection is provided by L, and this exemplifies the established strategy for imposition of unusually low coordination numbers, namely, enclosure of the metal by bulky substituents on the ligand. Thus, the two known methods for limiting Cu^{II} to three-coordination involve protective restriction by surrounding protein or by ligand bulk.

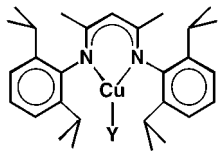

Scheme 1. CuLY complexes.

Here we report another effect that evidently restricts Cu^{II} to planar three-coordination with the smallest possible ligands, halide ions, as the species $[CuCl_xBr_{3-x}]^-$. This effect is enclosure of the anion in a hydrophobic domain of a lattice stabilised by interactions between polyatomic cations. The Cl^- and Br^- ligands provide no steric restriction to three-coordination, and the analogous three-coordinate halocuprate(I) complexes are well known.[6] Two crystalline compounds were characterised, both with the $[Ph_3PNPPh_3^+]$ ion,[7] namely, $(Ph_3PNPPh_3^+)[CuCl_{0.9}Br_{2.1}]^-$ (**1**), and $[Ph_3PNPPh_3^+][Cu-$

[a] C. Hasselgren, Prof. S. Jagner
Department of Inorganic Chemistry
Chalmers University of Technology
412 96 Göteborg (Sweden)
Fax: (+46) 31-7722846
E-mail: catrin@inoc.chalmers.se, susan@inoc.chalmers.se

[b] Prof. I. Dance
School of Chemistry
University of New South Wales
Sydney, NSW 2052 (Australia)
Fax: (+61) 2-9385-6141
E-mail: i.dance@unsw.edu.au

Supporting information for this article is available on the WWW under http://www.wiley-vch.de/home/chemistry/.

 © WILEY-VCH Verlag GmbH, 69451 Weinheim, Germany, 2002 0947-6539/02/0806-1270 $ 17.50+.50/0

$Cl_{2.4}Br_{0.6}]^-$ (**2**). The three coordination is unambiguous, as there is no other donor atom within 6.7 Å of the Cu centre. This is a molecular crystal, maintained by supramolecular interactions which are analogous energetically (but not chemically) to the stabilising interactions at the protein sites. The key question here is whether the supramolecular interactions in these molecular crystal lattices enforce the novel three-coordination of copper(II), just as the stabilising supramolecular interactions between $[MePh_3P^+]$ ions enforce the unique coordination chemistry of the anion $[Cu_2Br_5]^{2-}$.[8] In response to this question, we analyse the crystal supramolecularity of **1** and **2**, and of other relevant compounds.

Another aspect of the coordination chemistry of copper(II) in the type 1 blue copper proteins is weak coordination by a methionine sulfur atom.[2] We also report here the crystal structure of $[Ph_3PNPPh_3^+]$ $[CuCl_{0.7}Br_{2.3}(NCCH_3)]^-$ (**3**), in which acetonitrile is a fourth weak ligand for three-coordinate $[CuCl_{0.7}Br_{2.3}]^-$.

When X is a ligand with bridging capability, $[M^{II}X_3]^-$ normally occurs as dimetallic $[X_2M(\mu\text{-}X)_2MX_2]^{2-}$ to achieve four-coordination (tetrahedral or planar) at M. Thus with Cl^- and Br^- as the only ligands, the complexes $[Cu_2Cl_6]^{2-}$ and $[Cu_2Br_6]^{2-}$ could be expected. In the context of the unusual crystals **1** and **2** involving the cation $[Ph_3PNPPh_3]^+$, the question arises why the alternative complexes with four-coordinate copper(II), crystallised as $[Ph_3PNPPh_3^+]_2$-$[X_2CuX_2CuX_2]^{2-}$ (X = Cl or Br), did not form in the mixtures from which **1** and **2** crystallised. We address this question by reporting here also the different crystal structures of the homo-halo four-coordinate complexes $[Ph_3PNPPh_3^+]_2$-$[Cl_2CuCl_2CuCl_2]^{2-}$ (**4**), and $[Ph_3PNPPh_3^+]_2$ $[Br_2CuBr_2CuBr_2]^{2-}$ (**5**), and analysing their crystal supramolecularity. We also report the results of density functional calculations of the relevant intramolecular and intermolecular energies.

Experimental Section

$[Ph_3PNPPh_3]^+[CuCl_{0.9}Br_{2.1}]^-$ (1): $[Ph_3PNPPh_3]^+Cl^-$ (0.0475 g, 0.083 mmol) was dissolved in ethanol (25 mL), $CuBr_2$ (0.0185 g, 0.083 mmol) was added and the solution turned yellow-brown. Green-black crystals suitable for X-ray diffraction were grown by addition of CH_2Cl_2 to the solution (1:1) in a micro test tube (4 mL), followed by evaporation. Thin green-black plates of **1** formed after a few days.

$[Ph_3PNPPh_3]^+[CuCl_{2.4}Br_{0.6}]^-$ (2): $[Ph_3PNPPh_3]^+Cl^-$ (0.0471 g, 0.082 mmol) was dissolved in ethanol (25 mL), and $CuCl_2$ (0.0057 g, 0.042 mmol) and $CuBr_2$ (0.0095 g, 0.042 mmol) were added. The solution turned dark yellow, and 2 mL of this solution was placed in a micro test tube (4 mL), and CH_2Cl_2 (2 mL) added. Brown-black crystals formed upon evaporation after 9 d.

The halide ratios in **1** and **2** were determined from the refinement of the X-ray diffraction data, and the approximate ratios were substantiated by EDAX measurements on the relevant single crystals.

$[Ph_3PNPPh_3^+][CuCl_{0.7}Br_{2.3}(NCCH_3)]^-$ (3): $[Ph_3PNPPh_3]^+Cl^-$ (0.0492 g, 0.086 mmol) was dissolved in acetonitrile (25 mL). Addition of $CuBr_2$ (0.019 g, 0.086 mmol) with stirring resulted in a dark green-black solution. Black, needle-shaped crystals formed upon evaporation. The halide ratio was determined from the refinement of the X-ray diffraction data, and the approximate ratio was confirmed by EDAX measurements on the crystal used for data collection.

$[Ph_3PNPPh_3^+]_2[Cu_2Cl_6]^{2-}$ (4): $CuCl_2$ (0.0196 g, 0.146 mmol) was added to a solution of $[Ph_3PNPPh_3]^+Cl^-$ (0.0836 g, 0.146 mmol) in ethanol (20 mL). The solution changed colour from light green to a darker yellow-green. Dark green needles suitable for X-ray diffraction formed upon slow evaporation.

$[Ph_3PNPPh_3^+]_2[Cu_2Br_6]^{2-}$ (5): $[Ph_3PNPPh_3]^+Br^-$ (0.0177 g, 0.0286 mmol) was dissolved in ethanol (25 mL), and $CuBr_2$ (0.006 g, 0.0286 mmol) was added. The solution was stirred for a few minutes and then left to evaporate. Black, prismatic crystals (m.p. 156 °C) formed.

Further crystallisation experiments: The formation and crystallisation of **1** and **2** under different conditions was investigated. Alternative solvents added to the preparative mixture in ethanol were CCl_4, *n*-hexane, THF, cyclohexanol and diethyl ether, but in all cases the crystals formed were unsuitable for single-crystal X-ray diffraction. The preparation described above was also performed on a larger scale in ethanol, and with addition of

Table 1. Crystallographic data for **1**–**5**.

	[PNP][CuX_3] (**1**)	[PNP][CuX_3] (**2**)	[PNP][$CuX_3(NCCH_3)$] (**3**)	[PNP][Cu_2Cl_6] (**4**)	[PNP][Cu_2Br_6] (**5**)
formula	$C_{36}H_{30}P_2NCuBr_{2.1}Cl_{0.9}$	$C_{36}H_{30}P_2NCuBr_{0.6}Cl_{2.4}$	$C_{38}H_{33}P_2N_2CuBr_{2.3}Cl_{0.7}$	$C_{36}H_{30}P_2NCuCl_3$	$C_{36}H_{30}P_2NCuBr_3$
M_r [$g^{-1}mol^{-1}$]	802.7	735.3	850.14	708.4	841.8
crystal system	triclinic	triclinic	monoclinic	monoclinic	orthorhombic
space group	$P\bar{1}$	$P\bar{1}$	$C2/c$	$P2_1/c$	$Fddd$
a [Å]	10.000(2)	9.9690(6)	35.032(3)	9.2026(1)	15.3556(4)
b [Å]	11.258(4)	11.2737(11)	9.0719(4)	22.3956(2)	26.9512(8)
c [Å]	15.926(3)	15.9871(13)	23.124(2)	16.3270(1)	34.7035(15)
α [°]	73.28(2)	72.501(7)	90	90	90
β [°]	82.21(2)	81.814(7)	96.508(7)	103.198(1)	90
γ [°]	87.16(3)	87.598(7)	90	90	90
V [Å^3]	1701.2(7)	1696.1(2)	7301.6(9)	3276.1(1)	14362.1(8)
Z	2	2	8	4	16
ρcalcd [$g^{-1}cm^{-3}$]	1.57	1.44	1.55	1.44	1.56
λ [Å]	0.85	0.71073	0.71073	0.71073	0.71073
R_1	0.0749	0.0738	0.0487	0.0505	0.0647
wR_2	0.2076	0.2183	0.1007	0.1455	0.2185
GOF	0.691	1.027	0.992	0.976	1.011
no. of ind. reflections	6718	5963	6419	5751	3173
no. of ind. reflections ($I > 2\sigma(I)$)	2444	2939	3416	3783	1468
no. of parameters	392[a]	391	415	388	196
F(000)	802	748	3406	1452	6672
μ [mm^{-1}]	3.32	1.67	3.25	1.04	4.06
Max./min. residual electron density [e Å^{-3}]	1.4/ – 0.9	0.9/ – 0.8	0.6/ – 0.6	0.8/ – 0.6	1.6/ – 0.6

[a] Extinction coefficient refined.

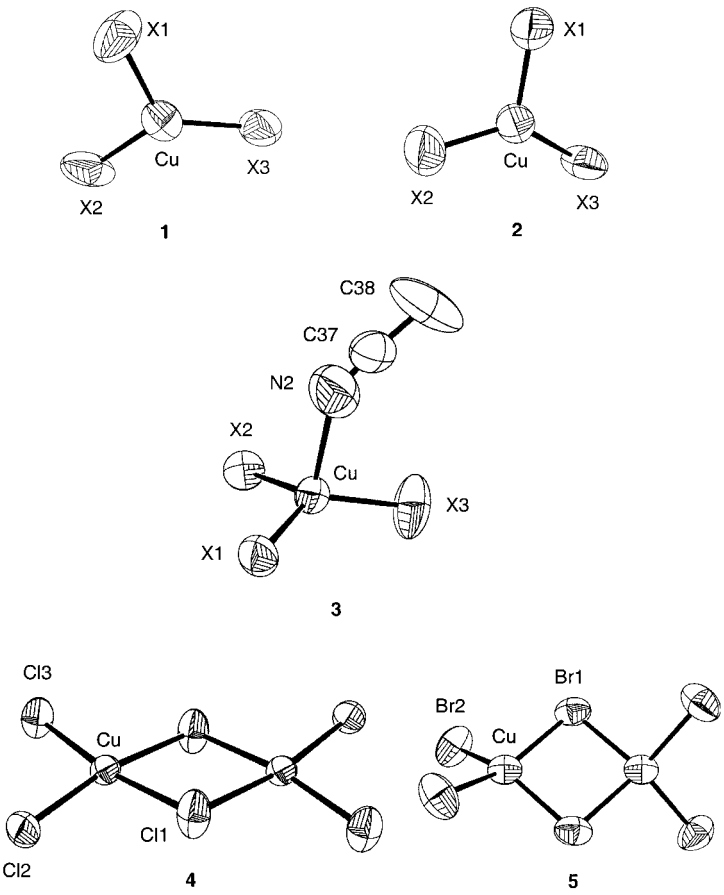

Figure 1. The molecular structures of the anions in **1**–**5**, with atom labels for the asymmetric unit (**4** is centrosymmetric and the centroid of **5** is at a 222 (D_2) site), and thermal ellipsoids at 50% probability. X1 is the Cl1/Br1 site, X2 is Cl2/Br2 and X3 is Cl3/Br3.

varying amounts of CH_2Cl_2, but did not yield suitable crystals. The mixture was prepared in the solvents nitromethane, methanol, *n*-propanol, and *n*-butanol, without the formation of suitable crystals. Reaction in acetonitrile yielded **3**. The ratio of $[Ph_3PNPPh_3]^+Cl^-$ and $CuBr_2$ was also varied, to 2:1 and 1:2, but it was not until $CuCl_2$ was added as well that any good crystals formed (**2**). Even with the successful method of crystallising **1** and **2**, it is difficult to obtain good crystals, and many batches instead contain unsuitable crystals. It also appears that the amount of CH_2Cl_2 is important, although most of the CH_2Cl_2 would probably have evaporated prior to crystallisation.

Crystal structure determinations: The crystals of **1**–**5** were cleaved prior to diffraction measurements. The diffraction data for **1** were collected with synchrotron X-ray vertical wiggler radiation at the MAX I711 beamline[9] in Lund by using the SMART-NT software.[10] Data reduction used SAINT+ and absorption correction used SADABS included in the SAINT+ package.[11] Diffraction data for compounds **2**–**5** were collected on an Enraf-Nonius CAD-4 diffractometer with $Mo_{K\alpha}$ radiation. Psi scans were used for absorption corrections for **2**–**4**, but no suitable reflections for psi scan correction were found for **5.** All structures were solved by direct methods (SHELXS) and refined with SHELXL.[12] Refinement of the disordered atoms was performed by refining one component of the site and resetting the other while constraining the total site occupancy to 1.0. Details of the structure determinations and refinements are compiled in Table 1. ORTEP plots of the five anions showing the atom labelling and the well-behaved thermal ellipsoids are shown in Figure 1. Atom occupancies and intramolecular dimensions are given in Tables 2 and 3. Crystallographic data (excluding structure factors) for the structures reported in this paper have been deposited with the Cambridge Crystallographic Data Centre as supplementary publication numbers CCDC-170690 (**1**), CCDC-170691 (**2**), CCDC-170692 (**3**), CCDC-170693 (**4**), and CCDC-170694 (**5**). Copies of the data can be obtained free of charge on application to CCDC, 12 Union Road, Cambridge CB2 1EZ, UK (fax: (+44) 1223-336-033; e-mail: deposit@ccdc.cam.ac.uk).

Table 3. Bond lengths [Å] and angles [°] for the anions of **4** and **5**.[a]

	[PNP][Cu_2Cl_6] (**4**)		[PNP][Cu_2Br_6] (**5**)
Cu1–Cl1	2.301(1)	Cu1–Br1^b (Å)	2.440(2)
Cu1–Cl2	2.216(1)	Cu1–Br2^t (Å)	2.326(2)
Cu1–Cl3	2.214(1)	Br1-Cu1-Br1^i	86.86(8)
Cu1–Cl1^{iii}	2.302(1)	Br1-Cu1-Br2	147.85(4)
Cl1-Cu1-Cl2	91.36(5)	Br1-Cu1-Br2^i	95.36(5)
Cl1-Cu1-Cl3	169.81(6)	Br2-Cu1-Br2^i	99.33(1)
Cl2-Cu1-Cl3	95.99(5)	Cu1-Br1-Cu1^{ii}	93.14(8)
Cl1-Cu1-Cl1^{iii}	82.10(5)		
Cl1^{iii}-Cu1-Cl2	170.90(6)		
Cl1^{iii}-Cu1-Cl3	91.31(5)		
Cu1-Cl1^{iii}-Cu1	97.90(5)		

[a] Symmetry codes: i: $x, -y+3/4, -z+3/4$; ii: $-x+3/4, -y+3/4, z$; iii: $2-x, -y, 2-z$. t = terminal, b = bridging.

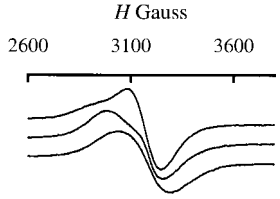

Figure 2. ESR spectrum of crystalline **1**. The sample was rotated between each recording.

ESR spectroscopy: An ESR spectrum of crystalline **1** is shown in Figure 2. The parameters for a frozen solution of **1** in ethanol are $g_x = 2.065$, $g_y = 2.085$, $g_z = 2.426$, $A_z = 114$ Gauss. Further investigations of the ESR and the electronic spectra of **1** are in progress.

Methods of calculation: Unrestricted density functional calculations were performed with numerical basis sets as implemented in the program DMol.[13] Our procedure for evaluation and validation of functionals (BLYP, VWN) for the present purposes involved calculation of the geometry and vibrational frequencies of $CuCl_2$,[14] and the geometries of $[Cu_2Cl_6]^{2-}$ and $[Cu_2Br_6]^{2-}$. Details are given in the Supporting Information. The conclusion is that, with numerical basis sets, the BLYP functional underestimates the strength of Cu^{II}–halide bonding by 0.10 to 0.14 Å, while the VWN functional calculates bond lengths with an accuracy of 0.01 Å. In previous work,[15] we showed that the VWN functional slightly overestimates intermolecular energies, and that VWN-calculated intermolecular energies scaled by 0.7 yield experimental energies for arene ··· arene in-

Table 2. Bond lengths [Å], bond angles [°] and atom occupancies for the anions of **1**–**3**.

	[PNP][CuX_3] (**1**)		[PNP][CuX_3] (**2**)		[PNP][$CuX_3(NCCH_3)$] (**3**)	
		X = Cl/Br		X = Cl/Br		X = Cl/Br
Cu–X1	2.263(2)	0.11(1)/0.89(1)	2.163(2)	0.77(1)/0.23(1)	2.292(1)	0.14(1)/0.86(1)
Cu–X2	2.164(2)	0.38(1)/0.62(1)	2.093(3)	0.86(1)/0.14(1)	2.238(1)	0.37(1)/0.63(1)
Cu–X3	2.226(2)	0.39(1)/0.61(1)	2.150(2)	0.76(1)/0.24(1)	2.211(1)	0.23(1)/0.77(1)
Cu–N2					2.439(8)	
X1-Cu1-X2	103.48(9)		108.52(1)		107.81(4)	
X1-Cu1-X3	118.89(7)		116.57(1)		119.56(4)	
X2-Cu1-X3	137.63(9)		134.91(1)		124.46(5)	
X1-Cu1-N2					105.63(2)	
X2-Cu1-N2					102.16(2)	
X3-Cu1-N2					91.91(2)	
Displ. of Cu from X_3 plane [Å]	0.002(1)		0.003(2)		0.372(1)	

 © WILEY-VCH Verlag GmbH, 69451 Weinheim, Germany, 2002 0947-6539/02/0806-1272 $ 17.50+.50/0 *Chem. Eur. J.* **2002**, *8*, No. 6

teractions. The BLYP functional cannot be used for intermolecular energies.[15, 16]

Results

Molecular structures of $[Cu(Cl/Br)_3]^-$ in 1 and 2: Crystals **1** and **2** are isostructural; both contain the trigonal-planar $[Cu(Cl/Br)_3]^-$ ion, but with differences in the disordered distribution of Cl and Br ligands. Figure 3 summarises the key

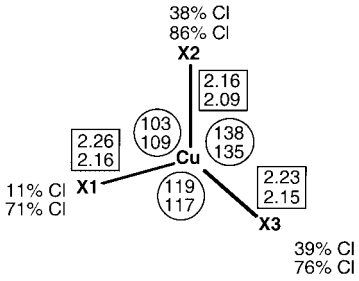

Figure 3. Summary of the molecular dimensions of the $[CuX_3]^-$ ions in **1** (upper values) and **2** (lower values). The percentages are occupancies at X1, X2, X3, values in rectangles are distances [Å], and encircled values are angles [°] marked.

compositional and geometrical properties of these two anions: the ligands are labelled X1, X2, X3. In **1** there is more Br than Cl at each ligand position, and vice versa for **2**. Each anion has one X-Cu-X angle 15–18° larger than 120°, and another 11–17° smaller than 120°. The variation in the Cu–X distances (2.09–2.26 Å) follows approximately the distribution of Cl/Br at each location. However, regression of the six observed distances in terms of one Cu–Cl distance (2.12 Å) and one Cu–Br distance (2.20 Å) indicates large statistical errors, which means that the Cu–X distances vary for both Cl and Br (the normal correlation of distance with opposite angle for distorted three-coordination also does not hold for the observations in Figure 3). This is consistent with the calculated flat potential for variation of the Cu coordination geometry described below.

Electronic structure and potential surface of $[CuClBr_2]^-$: Key questions about the electronic structure and the potential energy surface of these three-coordinate $[Cu(Cl/Br)_3]^-$ species were addressed with density functional calculations.

Figure 4 shows the relative energies of three different structures of planar $[CuClBr_2]^-$ with different angles. The C_{2v}

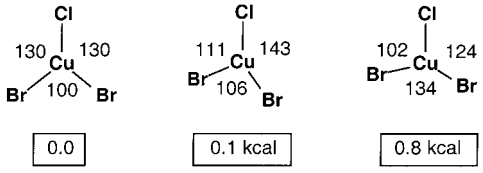

Figure 4. Relative energies [kcal mol^{-1}] for three planar forms of $[CuClBr_2]^-$ with the angles [°].

structure with angles of 130° (Cl-Cu-Br) and 100° (Br-Cu-Br) is less than 1 kcal mol^{-1} more stable than angularly distorted structures with Cl-Cu-Br angles down to 102° and Br-Cu-Br up to 134°, and it is clear that the energy surface for angle bending is very soft.

Figure 5 shows the orbital structure of $[CuClBr_2]^-$ as optimised with the VWN functional. The Cu 3d-based MOs are not widely differentiated by the halide ligands. The HOMO is an in-plane combination of Cu $3d_{xy}$ and Cu $3d_{x^2-y^2}$ orbitals, and there is a large gap to the LUMO. The relatively high energy of the HOMO indicates that $[CuClBr_2]^-$ is not unusually oxidised or susceptible to reduction to the formally Cu^I complex $[CuClBr_2]^{2-}$.

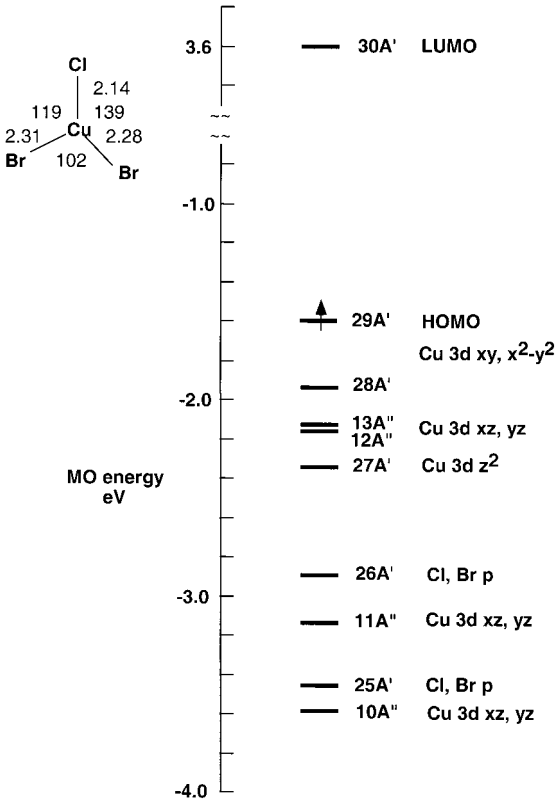

Figure 5. Molecular orbitals near the Fermi level for the optimised structure of $[CuClBr_2]^-$ as depicted, calculated with the VWN functional in symmetry C_s. This is a spin-restricted calculation; the results for the spin-unrestricted calculation are similar. Principal contributing atomic orbitals are identified. The HOMO is 29A′ with large contributions from the in-plane Cu $3d_{xy}$ and Cu $3d_{x^2-y^2}$ orbitals. The z axis is defined as perpendicular to the molecular plane.

Molecular structure of $[CuCl_{0.7}Br_{2.3}(NCCH_3)]^-$: The molecular structure of $[CuCl_{0.7}Br_{2.3}(NCCH_3)]^-$ in crystalline **3** is shown in Figure 6. The Cu atom has distorted trigonal-planar coordination, Cl and Br are disordered over the three halide ligand positions and the Cu atom is displaced 0.37 Å from the X_3 plane towards the more distant CH_3CN ligand. The secondary nature of the coordination to acetonitrile is shown by the elongation of the Cu–N distance by 0.45 Å relative to that of 1.99 Å in $[Cu(NCCH_3)_4]^+$, for instance.

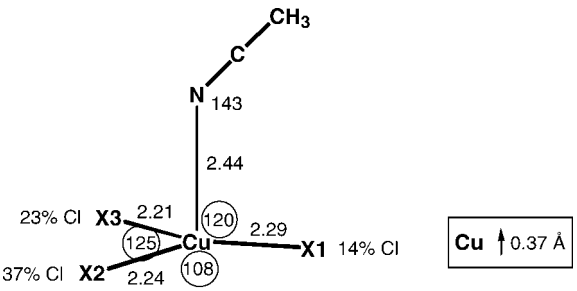

Figure 6. Dimensions [Å, °] of $[Cu(Cl/Br)_3(NCCH_3)]^-$ (**3**). The percentages are occupancies of Cl at the three halide ligand positions. The Cu atom is displaced 0.37 Å from the X_3 plane.

Electronic structure and potential energy surface of $[CuClBr_2(NCCH_3)]^-$: The electronic structure of **3** was investigated for $[CuClBr_2(NCCH_3)]^-$ (**3a**). The molecular orbitals (see Supporting Information) are unremarkable, with a HOMO (Cu 3d + Br 4p + Cl 3p) at −1.4 eV and a HOMO–LUMO gap of 3.5 eV. Of more significance is the potential energy surface for variation of the copper coordination environment between the planar three-coordinate $[CuClBr_2]^-$ and trigonal-pyramidal $[CuClBr_2(NCCH_3)]^-$. This energy variation, calculated as a function of the Cu–N axial distance with concomitant optimisation of the full coordination, is plotted in Figure 7. Variation of the copper coordination from compressed tetrahedral (Cu–$NCCH_3$ stronger than Cu–Cl/Br) through to the trigonal-planar structure represented by **1** and **2**, is accompanied by energy variation of less than 5 kcal mol^{-1}. This is a remarkable result. It further demonstrates the softness of the potential energy surface for copper(II) coordination with these ligands, and it indicates that analysis of any geometrical details of copper(II) coordination with such ligands is unimportant, because the energy changes are less than the supramolecular interaction energies of the complex with its surroundings. We analyse below the crystal packing and crystal supramolecular energies, and seek the reasons for stabilisation of **1** and **2**.

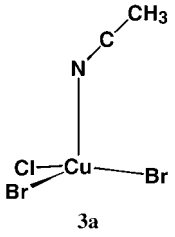

3a

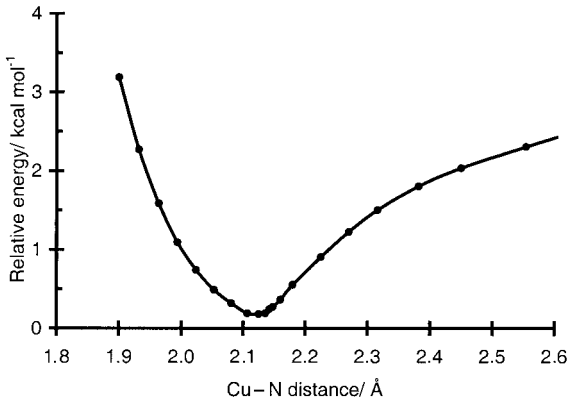

Figure 7. Calculated potential energy for axial coordination of $[CuClBr_2]^-$ by CH_3CN in **3a**. Variation of the Cu–N distances was accompanied by variation of the Cu coordination between compressed tetrahedral at the shortest Cu–N distance, to tetrahedral at the minimum, through axially extended pyramidal, to planar. Note that the associated energy changes are a few kilocalories per mole.

Molecular structures of $[Cu_2Cl_6]^{2-}$ and $[Cu_2Br_6]^{2-}$ in 5 and 6: The $[Cu_2Cl_6]^{2-}$ ion is centrosymmetric and almost planar, with Cl deviations from the best plane of 0.07 and 0.18 Å. The geometry of the $[Cu_2Br_6]^{2-}$ anion is midway between square-planar and tetrahedral (Figure 1). For distances and angles see Table 3. The DFT calculations confirm that the energy surface for bending within the anions is very flat, as is the case for the trigonally coordinated copper(II).

The crystal packing of 1 and 2: The crystal lattices of **1** and **2** are very similar (see Table 1), and are presented together. The space group is $P\bar{1}$, the unit cell is relatively small and almost equidimensional (10.0, 11.4, 16.2 Å; 72.7, 81.5, 87.2°) and the asymmetric unit contains one $[Ph_3PNPPh_3]^+$ ion, one $[CuX_3]^-$ ion and no solvent. In view of the disorder of Cl and Br, both within each of **1** and **2** and between their isomorphous lattices, the halides are labelled simply as X1, X2 and X3. The phenyl rings of the cation are differentiated in the figures as 1A, 1B, and 1C on P1, and 2A, 2B, and 2C on P2.

The lattice contains an approximately cubic array of $[CuX_3]^-$ anions, at $x \approx 0$, and most of the $[Ph_3PNPPh_3]^+$ material is located around $x = 1/2$, as shown in Figure 8. The unambiguous dispersal of the anions and the absence of interactions between them are demonstrated by the Cu ··· Cu distances, which are 8.1, 8.9, 10.0 and 11.4 Å, and the shortest interanion X ··· Cu distance of 6.73 Å.

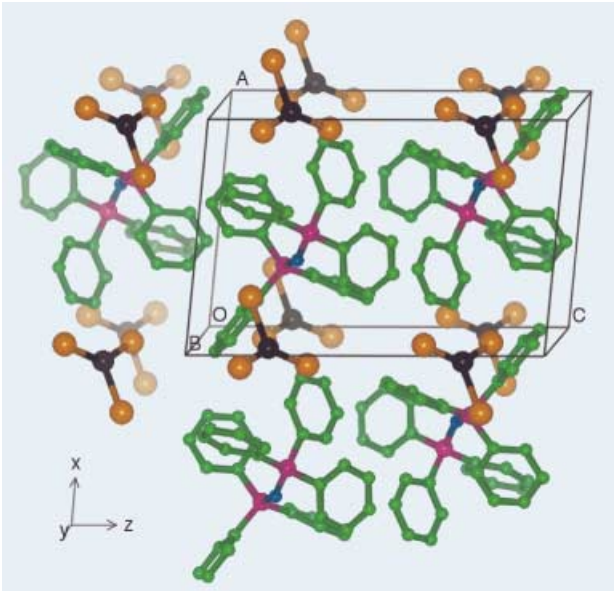

Figure 8. The arrangement of $[Ph_3PNPPh_3]^+$ ions and $[CuX_3]^-$ ions in **1**. The X atoms are brown, Cu black, C green, P magenta, N blue; H atoms are omitted. The separations between Cu atoms are 8.1 and 8.9 Å along *c*, 10.0 Å along *a* and 11.4 Å along *b*.

The stability of this lattice is the key question. We first evaluate all of the stabilising interactions between

 © WILEY-VCH Verlag GmbH, 69451 Weinheim, Germany, 2002 0947-6539/02/0806-1274 $ 17.50+.50/0 *Chem. Eur. J.* **2002**, *8*, No. 6

$[Ph_3PNPPh_3]^+$ ions, and then examine the interactions between cations and anions. The most prominent interaction between $[Ph_3PNPPh_3]^+$ ions occurs at the centre of the unit cell (and at the centre of an approximate cube of anions), around the centre of inversion at (1/2, 1/2, 1/2). This is a multiple-phenyl embrace involving six phenyl rings, 1A and 1B from one end and 2A from the other end of each cation, engaged in six edge-to-face (EF) local motifs, as shown in Figure 9. This embrace occurs in other crystals containing $[Ph_3PNPPh_3]^+$ and was described previously as a parallel expanded phenyl embrace.[17]

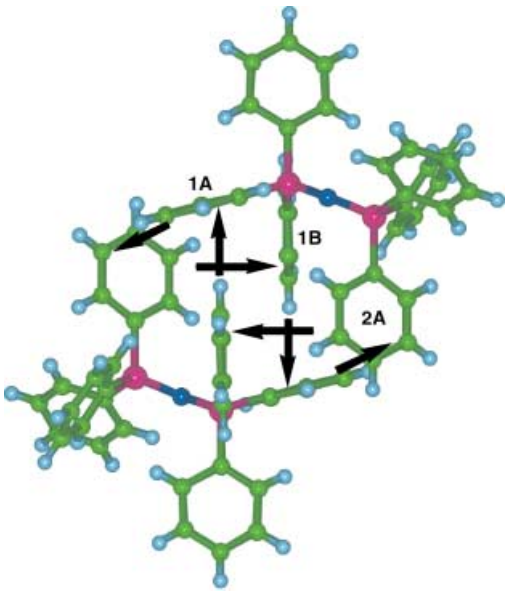

Figure 9. The centrosymmetric multiple-phenyl embrace of two $[Ph_3PNPPh_3]^+$ ions at (1/2, 1/2, 1/2) in **1**. The embrace comprises six edge-to-face (EF) interactions, marked with arrows.

Complete description of the cation $\cdots$ cation interactions in the crystal can be achieved by examining the surroundings of the other centres of inversion. Two cations form a good pair of EF interactions involving phenyl rings 1C and 2B at (1/2, 0, 0). The centres of inversion at (1/2, 0, 1/2) support a poor offset face-to-face (OFF) interaction, and there is no phenyl embrace around the inversion centre at (1/2, 1/2, 0). A full list of the phenyl $\cdots$ phenyl local motifs—1A EF to 2A′, 1A OFF to 1A′, 1B EF to 1A′, 1C EF to 2B′, 2A EF to 1B′, and 1C EF to 2C (intracation)—shows that all phenyl rings except 2C are involved in at least one good attractive intercation interaction. We conclude from this that the packing of the $[Ph_3PNPPh_3]^+$ ions in this crystal is efficient (there is no included solvent, which is sometimes evidence of poorer packing), and that intercation motifs contribute appreciably to the lattice stabilisation. Note that the net interaction between polyatomic cations such as $[Ph_3PNPPh_3]^+$ is attractive and stabilising: the van der Waals stabilisation at the optimum separation exceeds any coulombic destabilisation.

Having described the $[Ph_3PNPPh_3]^+ \cdots [Ph_3PNPPh_3]^+$ motifs occurring at $x = 1/2$, we now examine the anions and their surroundings in the vicinity of $x = 0$. As is evident from Figure 8, centres of inversion occur between all pairs of anions, and so the anions are parallel. There are no cations centred between these anions, but phenyl rings of the cations do protrude close to the interanion spaces. Specific C–H $\cdots$ X interactions occur between $[CuX_3]^-$ and the surrounding cations. Each of the three Cl/Br atoms has three immediately neighbouring H atoms at distances up to 3.3 Å and a number of slightly longer H $\cdots$ X contacts (Figure 10); the H $\cdots$ X

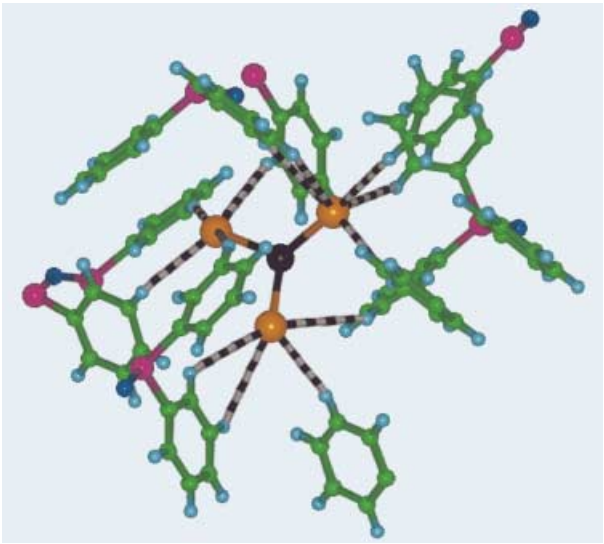

Figure 10. The immediate surrounding of a $[CuX_3]^-$ ion by phenyl rings of $[Ph_3PNPPh_3]^+$ ions in **1**. The more significant C–H $\cdots$ X contacts are marked with black and white stripes.

vectors are mainly close to the CuX_3 plane. Further, the principal H $\cdots$ X distances (C–H $\cdots$ X angles) of 3.04 (154), 3.09 (137), 3.17 (137) for X1; 2.76 (161), 3.08 (125), 3.19 (140) for X2; and 2.94 (142), 3.00 (139), 3.17 Å (138°) for X3 indicate energetically significant interactions between the anion and cation: the variations in distance are consistent with the flat region of the stabilising van der Waals potential, and the prevalence of C–H $\cdots$ X angles near 140° is noteworthy.

Intermolecular energies: The preceding analyses of geometry lead to the general conclusion that the crystal lattice of **1** (and **2**) is an effective capsule for the three-coordinate $[CuX_3]^-$ ion, which is stabilised within it by C–H $\cdots$ Cl/Br interactions. However, the key questions about the trapping and stabilisation of $[CuX_3]^-$ involve energies rather than geometries. We performed density functional calculations of intermolecular energy using the VWN and PWC functionals previously tested and calibrated for weaker intermolecular energies.[15, 16] The errors known to occur for such calculations on charged species were avoided by internal isoelectronic substitution, which has little effect on the charge distribution of polyatomic molecules and on the resulting intermolecular energies. Thus $[Ph_3PNPPh_3]^+$ was calculated as Ph_3PCPPh_3, and $[CuX_3]^-$ as GaX_3.

The calculated van der Waals energy for two Ph_3PCPPh_3 adopting the main embrace of two $[Ph_3PNPPh_3]^+$ shown in Figure 9 was calculated by DF methods to be – 18.3 kcal{mol

$(Ph_3PCPPh_3)_2\}^{-1}$. This is consistent with the known energy of about -2 kcal mol^{-1} per pair of benzene molecules. We know that the coulombic destabilisation for $[Ph_4P^+]_2$ in similar embraces is about 5 kcal mol^{-1}, and therefore, since the positive charge density on the surface of $Ph_3PNPPh_3^+$ is less than that of $[Ph_4P]^+$, the magnitude of the net stabilisation of the main $[Ph_3PNPPh_3^+]_2$ embrace (Figure 9) is estimated to be about -13 kcal mol^{-1}. This agrees with our previous estimates (using tested intermolecular potentials) that the energies of embracing $[Ph_3PNPPh_3]^+$ are in the range of -9 to -13 kcal mol^{-1}.[17]

The intermolecular energies between the anion in **1** and its surrounding cations was calculated by DFT methods for an assembly of six benzene molecules around $GaCl_3$ (or $GaBr_3$) in the same conformation as the immediate environment in the crystal (Figure 10; the assembly is shown in the Supporting Information). Each of these benzene molecules forms one or two definite C–H···X interactions with the halogen ligands. The calculated net intermolecular energy between $GaCl_3$ and the $(C_6H_6)_6$ assembly is -8 kcal mol^{-1} (VWN functional), and between the $GaBr_3$ and the $(C_6H_6)_6$ assembly -9 kcal mol^{-1} (VWN). For $[Ph_3PNPPh_3]^+\cdots[CuX_3]^-$ interactions a small coulombic stabilisation will enhance these values.

The general and semiquantitative conclusion from these calculations is that in **1** and **2** each Ph···Ph interaction contributes about 1.5 kcal mol^{-1} to the lattice stabilisation, and that each Ph···X interaction also contributes about 1.5 kcal mol^{-1} to the lattice stabilisation. The geometrical analysis of the crystal packing indicates that these stabilisations work in concert, and that all aspects of the crystal packing stabilise the unusual $[CuX_3]^-$ ions.

Crystal packing of 3, 4 and 5: Because compounds **3**, **4** and **5** occur as alternatives to **1** and **2**, it is important to assess the alternative crystal packing that they exhibit. We present here some principal features, and will publish separately full analyses of the crystal packing.

Figure 11, a projection of the crystal structure of **3** along the shortest axis ($b = 9.1$ Å), shows a well-developed three-dimensional network of embraces between $[Ph_3PNPPh_3]^+$ cations, with channels which contain the $[CuX_3NCCH_3]^-$ ions. Along these channels the complex anions are well-separated, and linked by C–H···X interactions, as shown in Figure 12. In addition, there are many (Ph)C–H···X interactions in **3**, not unlike those in **1** (Figure 10).

Compound **4**, $[Ph_3PNPPh_3^+]_2[Cu_2Cl_6]$, crystallises in the space group $P2_1/c$. The crystal lattice consists of waves of cations engaged in unconventional embraces. Cations encapsulate centrosymmetric $[Cu_2Cl_6]^{2-}$ ions in a pseudocubic manner with multiple C–H···Cl interactions, as illustrated in Figure 13.

Compound **5**, $[Ph_3PNPPh_3^+]_2[Cu_2Br_6]^{2-}$, crystallises in the space group *Fddd* with a network of embracing cations that surround cavities containing the $[Cu_2Br_6]^{2-}$ ions with many C–H···Br interactions. Key motifs in the structure are shown in Figure 14.

Thus, it can be seen that the crystal packings of **3**, **4** and **5** are all different in detail, but manifest the same general principles. All possess cation-embrace motifs; all have well separated anions; all have well-developed C–H···X interactions; and all are devoid of lattice solvent molecules. It can be expected that the intermolecular energies for the $[Ph_3PNPPh_3]^+\cdots[Ph_3PNPPh_3]^+$ embrace motifs and for the C–H···X interactions will be similar to those calculated (see above) for **1** and **2**. On the basis of the packing and energy analysis there is no reason to believe that any of these crystal structures **1**–**5** has a marked stability advantage.

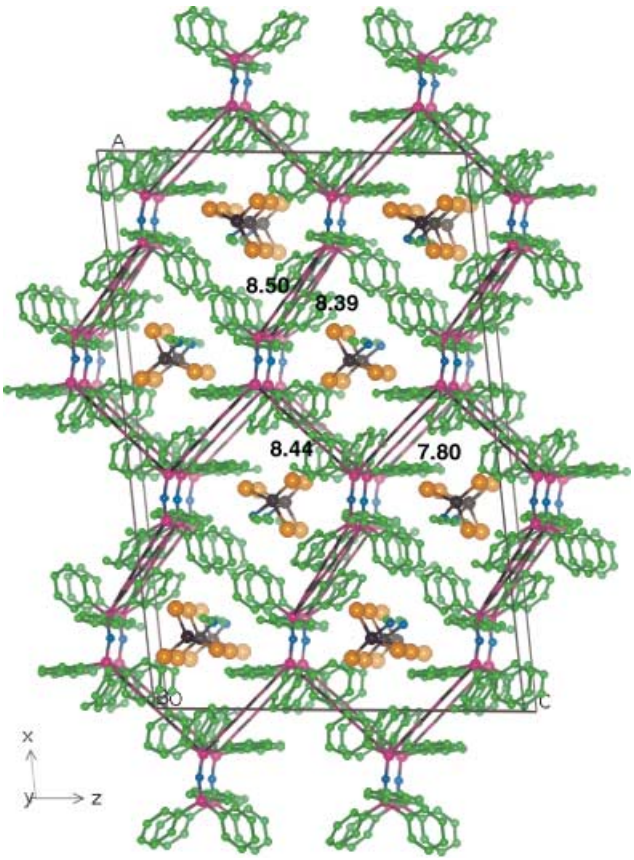

Figure 11. Projection of the crystal packing of $[Ph_3PNPPh_3]^+[CuX_3NCCH_3]^-$ (**3**) along the shortest axis ($b = 9.1$ Å) in the space group *C*2/*c*. The three-dimensional net of PNP···PNP motifs is indicated by the P···P connectors (magenta and black candystripes), which occur as four types with P–P distances of 7.80, 8.44, 8.39 and 8.50 Å. The $[CuX_3NCMe]^-$ ions are well separated along channels in the cation net.

Figure 12. The chain of $[CuX_3NCCH_3]^-$ ions in **3**. The H–X distances of the C–H···X interactions (black and white stripes) are 3.37 and 3.45 Å.

Discussion

We have shown that crystallisation from ethanol solutions containing copper(II) and the elementary chloride and bromide ligands, together with the

© WILEY-VCH Verlag GmbH, 69451 Weinheim, Germany, 2002
0947-6539/02/0806-1276 $ 17.50+.50/0 *Chem. Eur. J.* **2002**, *8*, No. 6

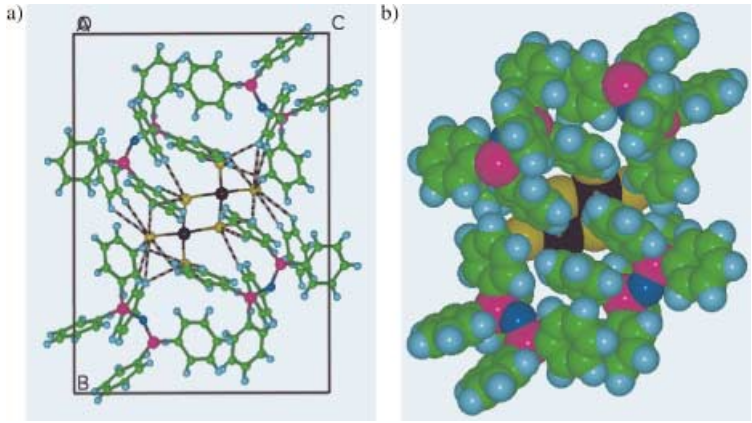

Figure 13. Eight $[Ph_3PNPPh_3]^+$ ions surround a $[Cu_2Cl_6]^{2-}$ ion in **4**, space group $P2_1/c$. In addition to the four $[Ph_3PNPPh_3]^+$ that are evident, four $[Ph_3PNPPh_3]^+$ are translated behind the anion. a) The black and white stripes identify the 26 C–H···Cl interactions (H···Cl ⩽ 3.2 Å) between $[Cu_2Cl_6]^{2-}$ and surrounding cations. b) The space-filling representation allows identification of the multiple pairs of approximately parallel phenyl rings.

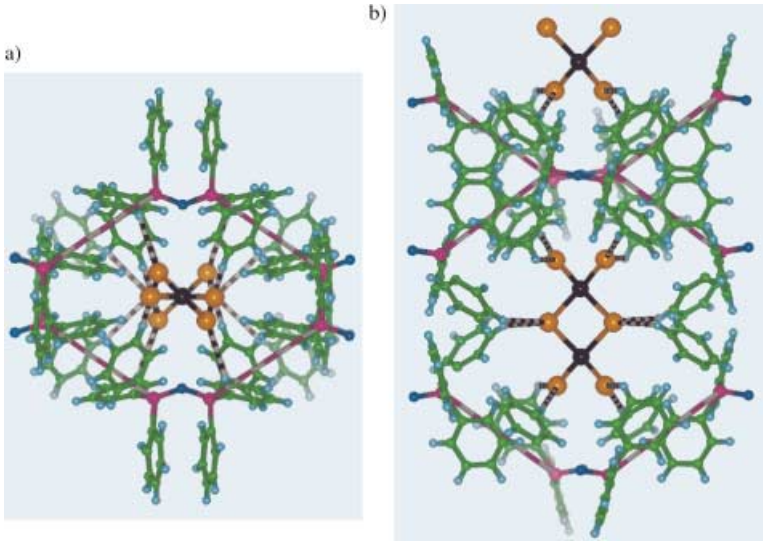

Figure 14. Cages of embracing $[Ph_3PNPPh_3]^+$ ions surrounding $[Cu_2Br_6]^{2-}$ ions in **5**. Parallel fourfold phenyl embraces between $[Ph_3PNPPh_3]^+$ ions are marked with magenta and white stripes, and C–H···Br interactions (H···Br ⩽ 3.3 Å) as black and white stripes: each Br has two C–H···Br interactions. Views along (a) and perpendicular (b) to sequences of $[Cu_2Br_6]^{2-}$ ions.

ligands, monatomic halide ions, provide further insight into the relative inherent stabilities of coordination numbers for Cu^{II}, and it can be concluded that three is a normal coordination number for Cu^{II}, and that previous occurrences need not be regarded as abnormal. With halide ligands it appears that the coordination preferences of Cu^{II} are not very different from those of Cu^{I}. There is weak EXAFS evidence for $[CuBr_3]^-$ in aprotic media.[18]

The $[Ph_3PNPPh_3]^+$ ions are evidently favourable in this demonstration of alternative coordination complexation by Cu^{II}, and we have identified the significance of the stabilising intercation embrace motifs and the numerous C–H···X interactions with the halocuprate(II) complexes. In this context we draw attention to another report, obscure and previously unrecognised, of the $[CuCl_3]^-$ anion stabilised in a crystal lattice by similar crystal supramolecular interactions. This occurs in the compound $[GdCl_2(OPPh_3)_4]^+[CuCl_3]^-$, crystallised (Cambridge structural database refcode GEXRIK) from dichloromethane.[19] This compound crystallises in the space group $P\bar{1}$ with two formula units per asymmetric unit. The two independent $[CuCl_3]^-$ ions are planar but with different dimensions, as shown in Figure 15. Full analysis of the crystal packing[20] reveals that each of the $[CuCl_3]^-$ anions is encapsulated by a cage of phenyl groups on the peripheries of the cations, with well-developed C–H···Cl interactions (see Figure 16).

$[Ph_3PNPPh_3]^+$ ion, can yield three- and four-coordinate Cu^{II} halide complexes, and in the presence of CH_3CN (3 + 1)-coordinate copper(II) is formed. Four different molecular crystal lattices occur, albeit with similar crystal packing principles. From the perspective of the crystallisation conditions there appears to be little difference in stability between these related complexes with different coordination numbers, and this conclusion is supported by the calculated intermolecular energies. We have not yet resolved the question of the apparent requirement for mixed chloride and bromide ligands in the stabilisation of $[CuX_3]^-$, but we suspect that the crystallisation of homoleptic $[CuCl_3]^-$ or $[CuBr_3]^-$ in the lattice of **1** or **2** is possible.

It is clear that this simple preparative mixture can be used to crystallise the uncommon three-coordinate Cu^{II}, and that it is not necessary to deploy enforcing ligands to control the coordination number and stereochemistry. Indeed, the solution and crystallisation behaviour with the simplest of

All of these results indicate that the deployment of cations with hydrophobic phenylated surfaces is favourable for the stabilisation and crystallisation of halocuprate(II) anions with

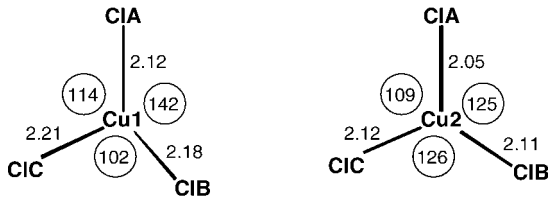

Figure 15. Dimensions [Å, °] of the two planar $[CuCl_3]^-$ ions in $[GdCl_2(OPPh_3)_4]^+[CuCl_3]^-$ (CSD GEXRIK).

 © WILEY-VCH Verlag GmbH, 69451 Weinheim, Germany, 2002 0947-6539/02/0806-1277 $ 17.50+.50/0

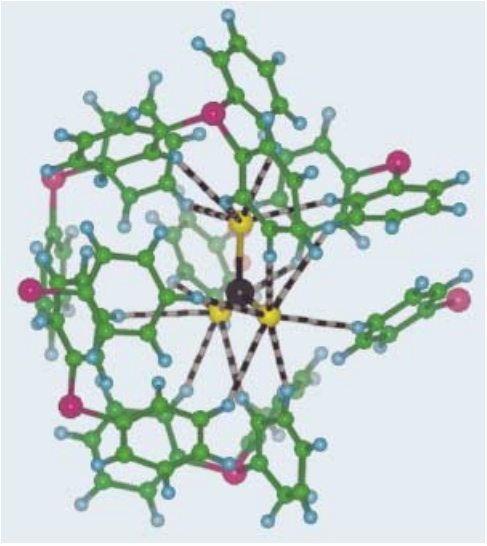

Figure 16. The surrounding phenyl groups and C–H···Cl interactions (black and white stripes) for one of the $[CuCl_3]^-$ ions in $[GdCl_2(OPPh_3)_4]^+[CuCl_3]^-$ (CSD GEXRIK).

unusual copper coordination. Such cations have stabilised other unusual stereochemistries and redox states in bromocuprate anions.[8, 21] However, considerable experience with similar cations shows that the presence of hydrophobic phenylated surfaces is not a sufficient condition for stabilisation of unusual coordination.

The major conclusion from this work is that these alternative coordination stereochemistries for copper(II) should not be regarded as abnormal. We reiterate the calculated energy potential for $Cu^{II}X_3-NCCH_3$ coordination (Figure 7), in which the full range of coordination between tetrahedral and trigonal planar involves intramolecular energy variations of less than 5 kcal mol^{-1}, and less than the intermolecular energies. These results provide a relevant background for similar considerations of the energy-coordination stereochemistry surface for Cu^{II} and Cu^{I} in the blue type 1 copper proteins, particularly since the cysteine ligands are pseudohalides.

Acknowledgement

We thank Dr. Roland Aasa, Dept. of Molecular Biotechnology, Chalmers University of Technology, for carrying out the ESR measurements. This research has been supported by The Swedish Research Council (Natural and Engineering Sciences (VR/NFR)), Chalmers University of Technology, The Royal Society of Arts and Sciences in Gothenburg (KVVS), the Australian Research Council and the University of New South Wales.

[1] E. N. Baker in *Encyclopedia of Inorganic Chemistry* (Ed.: R. B. King), Wiley, New York **1994**, pp. 883–905.
[2] P. Comba, *Coord. Chem. Rev.* **2000**, *200–202*, 217–245.
[3] S. Alvarez, *Coord. Chem. Rev.* **1999**, *193–195*, 13–41.
[4] P. L. Holland, W. B. Tolman, *J. Am. Chem. Soc.* **1999**, *121*, 7270–7271.
[5] D. W. Randall, S. D. George, P. L. Holland, B. Hedman, K. O. Hodgson, W. B. Tolman, E. I. Solomon, *J. Am. Chem. Soc.* **2000**, *122*, 11632–11648.
[6] S. Jagner, G. Helgesson, *Adv. Inorg. Chem.* **1991**, *37*, 1–45.
[7] $[Ph_3PNPPh_3]^+$ is the bis(triphenylphosphoranylidene)ammonium ion.
[8] C. Horn, I. G. Dance, D. Craig, M. L. Scudder, G. A. Bowmaker, *J. Am. Chem. Soc.* **1998**, *120*, 10549–10550.
[9] Y. Cerenius, K. Ståhl, L. A. Svensson, T. Ursby, Å. Oskarsson, J. Albertsson, *J. Synchrotron Rad.* **2000**, *7*, 203–208.
[10] v. SMART-NT, Bruker AXS Inc. Madison, Wisconsin, USA, **1999**.
[11] v. SAINT+, Bruker AXS Inc. Madison, Wisconsin, USA, **1999**.
[12] G. M. Sheldrick, University of Gottingen, Germany, **1997**.
[13] B. Delley, *J. Chem. Phys.* **1990**, *92*, 508–517.
[14] B. K. Ystenes, V. R. Jensen, *Inorg. Chem.* **1999**, *38*, 3985–3993.
[15] S. Lorenzo, G. R. Lewis, I. G. Dance, *New J. Chem.* **2000**, *24*, 295–304.
[16] T. A. Wesolowski, O. Parisel, Y. Ellinger, J. Weber, *J. Phys. Chem.* **1997**, *101*, 7818–7825.
[17] G. R. Lewis, I. G. Dance, *J. Chem. Soc. Dalton Trans.* **2000**, 299–306.
[18] G. Kickelbick, U. Reinohl, T. S. Ertel, A. Weber, H. Bertagnolli, K. Matyjaszewski, *Inorg. Chem.* **2001**, *40*, 6–8.
[19] W. Xukun, Z. Mingjie, W. Jitao, *Jiegou Huaxue (J. Struct. Chem.)* **1988**, *7*, 142–147.
[20] I. G. Dance, unpublished results.
[21] G. A. Bowmaker, P. D. W. Boyd, C. E. F. Rickard, M. L. Scudder, I. G. Dance, *Inorg. Chem.* **1999**, *38*, 5476–5477.

Received: September 27, 2001 [F3580]

 © WILEY-VCH Verlag GmbH, 69451 Weinheim, Germany, 2002 0947-6539/02/0806-1278 $ 17.50+.50/0